

DISTRIBUTION OF DYNAMIC AND THERMAL STATISTICAL CHARACTERISTICS IN TURBULENT NON-ISOTHERMAL INCOMPRESSIBLE FLOWS IN A CYLINDRICAL TUBE ROTATING RELATIVE TO ITS AXIS

O. G. MARTYNENKO, I. A. VATUTIN and I. V. SKUTOVA

The Luikov Heat and Mass Transfer Institute, Byelorussian Academy of Sciences, Minsk, U.S.S.R.

(Received 5 April 1976)

Abstract—An effect is considered of a cylindrical tube rotation relative to its axis on distribution of the averaged velocity, temperature as well as tensor components of the Reynolds stresses, pulsation heat fluxes and RMS value of temperature fluctuations in an incompressible flow through a tube under forced motion conditions. Investigation is carried out by numerical solution of the system of non-linear differential equations. Discussion of the obtained results is presented.

NOMENCLATURE

- U , = $\frac{V_z}{v_*}$, averaged velocity;
- U_0 , averaged velocity on the tube axis;
- u_i , velocity pulsation;
- v_* , dynamic velocity;
- R_{ij} , = $\frac{\langle u_i u_j \rangle}{v_*^2}$, tensor components of the Reynolds stresses;
- δ_{ij} , Kronecker symbol;
- K , = $\sqrt{E} = \sqrt{[\frac{1}{2}(R_{11} + R_{22} + R_{33})]}$;
- l , L/a , turbulence scale;
- a , tube radius;
- R_{mean} , Reynolds number for mean mass velocity;
- R_* , = $\frac{av_*}{v}$, Reynolds number for dynamic velocity;
- Pr , Prandtl number;
- Θ , = $\frac{T_w - T}{T}$, relative temperature;
- T_w , wall temperature;
- T_* , = $\frac{q_w}{\rho C_p v_*}$, q_w , heat flux through a wall;
- $R_{u,t}$, = $\frac{\langle u_i t \rangle}{v_* T}$, t , temperature fluctuation;
- R_{tt} , = $\frac{\langle t^2 \rangle}{T^2}$.

formulas to predict turbulent friction and pulsation energy components for a fully developed and steady-state flow in a rotating tube. The main consideration has been given to investigation of the flow rotation effect on the critical Reynolds number. Levin's calculations have revealed that rotation decreases turbulent friction and due to the tendency to laminarization at an increasing rotation Reynolds number, $R_\omega = \omega a^2 / \nu$, the averaged velocity profile becomes less continuous. With non-isothermal flow rotation, one may expect transformation of the temperature profile and, therefore, of pulsation heat fluxes and of mean square temperature fluctuations. This is the very problem which will be treated in more detail in the present paper (with the diffusion terms in second moment equations taken into account).

At a sufficient distance from the tube inlet the averaged statistical flow characteristics (except pressure) vary only over a radius. A system of equations for the averaged velocity and tensor components of the Reynolds stresses in a cylindrical system of coordinates takes the form

$$-\frac{R_\omega^2}{R^2} r + \frac{1}{r} (R_{22} - R_{33}) + \frac{d}{dr} R_{22} = -\frac{1}{R^2} \frac{\partial \bar{P}}{\partial r}; \quad (1)$$

$$\frac{1}{r} \frac{d}{dr} (r R_{23}) + \frac{1}{r} R_{23} = -\frac{1}{r} \frac{1}{R^2} \frac{\partial \bar{P}}{\partial \varphi}; \quad (2)$$

$$\frac{1}{R} \left[\frac{1}{r} \frac{d}{dr} \left(r \frac{dU}{dr} \right) \right] - \frac{1}{r} \frac{d}{dr} (r R_{12}) = \frac{1}{R^2} \frac{\partial \bar{P}}{\partial z}; \quad (3)$$

$$R_{12} \frac{dU}{dy} + c \frac{K^3}{l} + c_1 \frac{1}{R} \frac{K^2}{l^2} - \frac{1}{R} \frac{1}{r} \frac{d}{dr} \left(r \frac{d}{dr} K^2 \right) - \frac{1}{R_*} \left[-\frac{1}{r^2} (R_{22} + R_{33}) \right] - B_1 \left[\frac{d}{dr} \left(\sqrt{(R_{22})l} \frac{dK^2}{dr} \right) + \frac{1}{r} \sqrt{(R_{22})l} \frac{d}{dr} K^2 \right] - 2B_2 \sqrt{2} \frac{d}{dr} \left(Kl \frac{d}{dr} R_{22} \right) = 0; \quad (4)$$

THE QUALITATIVE considerations are known [1] concerning a stabilizing effect of centrifugal forces on turbulence. Proceeding from the equations for dynamic statistical characteristics in non-diffusional approximation (contribution of viscous diffusion, turbulent diffusion and pressure diffusion being neglected) and employing the Prandtl-Nikuradze mixing length as a turbulence scale, Levin [2] has derived approximate

$$R_{22} \frac{dU}{dr} + K_p \frac{K}{l} R_{12} + \frac{1}{R_*} c_1 \frac{R_{12}}{l^2} - \frac{1}{R_*} \left(\frac{d^2}{dr^2} R_{12} + \frac{1}{r} \frac{d}{dr} R_{12} - \frac{1}{r^2} R_{12} \right) + B_1 \left[\frac{d}{dr} \left(\sqrt{(R_{22})l} \frac{d}{dr} R_{12} \right) + \frac{1}{r} \sqrt{(R_{22})l} \frac{d}{dr} R_{12} \right] + B_2 \sqrt{2} \frac{d}{dr} \left(Kl \frac{d}{dr} R_{12} \right) - 2R_{13} \frac{R_\omega}{R_*} = 0 \quad (5)$$

$$2R_{12} \frac{dU}{dr} + K_p \frac{K}{l} (R_{11} - \frac{2}{3} K^2) + \frac{2}{3} c \frac{K^3}{l} + \frac{c_1 R_{11}}{R_* l^2} - \frac{1}{R_*} \frac{1}{r} \frac{d}{dr} \left(r \frac{d}{dr} R_{11} \right) - B_1 \left[\frac{d}{dr} \left(\sqrt{(R_{22})l} \frac{d}{dr} R_{11} \right) - \frac{1}{r} \sqrt{(R_{22})l} \frac{d}{dr} R_{11} \right] = 0; \quad (6)$$

$$K_p \frac{K}{l} (R_{33} - \frac{2}{3} K^2) + \frac{2}{3} c \frac{K^3}{l} + \frac{c_1 R_{33}}{R_* l^2} - \frac{1}{R_*} \left(\frac{d^2}{dr^2} R_{33} + \frac{1}{r} \frac{d}{dr} R_{33} - \frac{2}{r^2} R_{33} \right) - B_1 \left[\frac{d}{dr} \left(\sqrt{(R_{22})l} \frac{d}{dr} R_{33} \right) + \frac{3}{r} \sqrt{(R_{22})l} \frac{d}{dr} R_{33} \right] + 4R_{23} \frac{R_\omega}{R_*} = 0; \quad (7)$$

$$R_{22} = 2K^2 - (R_{11} + R_{33}); \quad (8)$$

$$R_{23} \frac{dU}{dr} + K_p \frac{K}{l} R_{13} + \frac{1}{R_*} c_1 \frac{R_{13}}{l^2} - \frac{1}{R_*} \left(\frac{d^2}{dr^2} R_{13} + \frac{1}{r} \frac{d}{dr} R_{13} - \frac{1}{r^2} R_{13} \right) + B_1 \left[\frac{d}{dr} \left(\sqrt{(R_{22})l} \frac{d}{dr} R_{13} \right) + \frac{2}{r} \sqrt{(R_{22})l} \frac{d}{dr} R_{13} \right] + 2R_{12} \frac{R_\omega}{R_*} = 0; \quad (9)$$

$$K_p \frac{K}{l} R_{23} + \frac{c_1 R_{23}}{R_* l^2} - \frac{1}{R_*} \left[\frac{1}{r} \frac{d}{dr} \left(r \frac{d}{dr} R_{23} \right) - \frac{2}{r^2} \left\langle \omega \frac{\partial \omega}{\partial \varphi} \right\rangle \right] + B_1 \left[\frac{d}{dr} \left(\sqrt{(R_{22})l} \frac{dR_{23}}{dr} \right) + \frac{2}{r} \sqrt{(R_{22})l} \frac{dR_{23}}{dr} \right] + B_2 \sqrt{2} \left[\frac{d}{dr} \left(Kl \frac{d}{dr} R_{23} \right) \right] - 2(R_{33} - R_{22}) \frac{R_\omega}{R_*} = 0; \quad (10)$$

$$l = 0.14 - 0.08r^2 - 0.06r^4. \quad (11)$$

When closing this system for correlations, involving pressure pulsations and velocity pulsation derivatives, as well as for dissipative functions the approximations suggested by Rotta [3] are used

$$\frac{1}{\rho} \left\langle P \left(\frac{\partial u_i}{\partial x_j} + \frac{\partial u_j}{\partial x_i} \right) \right\rangle = -k_p \frac{\sqrt{E}}{L} [\langle u_i u_j \rangle - \frac{2}{3} E \delta_{ij}], \quad (12)$$

$$2\nu \left\langle \frac{\partial u_i}{\partial x_k} \frac{\partial u_j}{\partial x_k} \right\rangle = \nu c_1 \frac{\langle u_i u_j \rangle}{L^2} + \delta_{ij} \frac{2}{3} c \frac{E^{3/2}}{L}. \quad (13)$$

where $k_p = 0.96$; $c = 0.18$; $c_1 = 5\pi/4$.

The functions, characterizing turbulent diffusion of the Reynolds stresses and diffusion due to pressure pulsations, are approximated according to Donaldson [4]:

$$\frac{\partial}{\partial x_k} \langle u_k u_i u_j \rangle = -B_1 \frac{\partial}{\partial x_k} [L \sqrt{\langle u_k^2 \rangle} \frac{\partial}{\partial x_k} \langle u_i u_j \rangle]; \quad (14)$$

$$\frac{1}{\rho} \left[\frac{\partial}{\partial x_i} \langle p u_j \rangle + \frac{\partial}{\partial x_j} \langle p u_i \rangle \right] = -B_2 \left[\frac{\partial}{\partial x_j} \left(L \sqrt{(2E)} \frac{\partial}{\partial x_i} \langle u_i u_i \rangle \right) + \frac{\partial}{\partial x_i} \left(L \sqrt{(2E)} \frac{\partial}{\partial x_i} \langle u_j u_i \rangle \right) \right]; \quad (15)$$

where $B_1 = 1.6$ and $B_2 = 0.12$ are the constants determined from the correlation which is of best fit for the predicted functions and the experimental data of Comte-Bellot [5] for a fully developed turbulent flow case in a plane channel. It should be borne in mind that in equations (14) and (15) summation over k is not expected in the multiplier $\sqrt{\langle u_k^2 \rangle}$.

Equations (1)-(11) are solved at the following boundary conditions

$$U|_{r=1} = R_{ij}|_{r=1} = 0; \quad (16)$$

$$\frac{d}{dr} U \Big|_{r=0} = \frac{d}{dr} R_{ij} \Big|_{r=0} = 0.$$

For each nonlinear differential equation the quasi-linearization method [6] and then the finite-difference procedure are employed. From the experimental data the desired functions are known to vary smoothly near the channel axis and possess a sharp maximum near the wall. In this connection, the entire range of integration is divided into 6 parts

$$0 \leq y_1 \leq 0.5; \quad 0.5 < y_2 \leq 0.6; \quad 0.6 < y_3 \leq 0.7;$$

$$0.7 < y_4 \leq 0.8; \quad 0.8 < y_5 \leq 0.9; \quad 0.9 < y_6 \leq 1;$$

and each of these intervals in their turn is subdivided into n equal portions with a different step h_m for each integration interval. For the first interval, $h_1 = 0.025$. For the remainder, a smaller step is chosen according to the geometric progression with a denominator of 1/2, i.e. $h_m = h_1 (\frac{1}{2})^{m-1}$. Further step refinement makes no sense since the results for the present step and the double-sized one do not differ more than by 10^{-4} . The system of algebraic equations is solved by the elimination method [7]. So, calculations proceed as follows: employing initial approximations for the unknown functions solution is obtained by the Gauss-Seidel method. As initial approximations, the function $\cos \pi \cdot 2 \cdot r$ is used which satisfies the boundary conditions (16). Iterations are performed till the condition $|f_{n-1} - f_n| < \varepsilon$ with $\varepsilon = 10^{-6} - 10^{-8}$ is fulfilled. The computation time of one run on the electronic computer "M-220" is 3-5 min.

With the known distribution of dynamic statistical characteristics over the tube cross-section, the averaged temperature, pulsation heat fluxes and mean square temperature fluctuations are predicted provided the heat flux through a wall is constant and a consideration is made of the region where $\partial T / \partial z = \text{const}$. The

appropriate equations are of the form

$$\frac{1}{PrR.} \frac{d\Theta}{dr} - R_{vt} = \frac{1}{r} \int_0^r \frac{Ur dr}{\int_0^1 Ur dr}; \quad (17)$$

$$R_{22} \frac{d\Theta}{dr} + \frac{1}{\int_0^1 Ur dr} R_{12} + 0.48 \sqrt{(Pr)K} \frac{R_{vt}}{l} + \pi \frac{1}{PrR.} \frac{R_{vt}}{l^2} - \frac{1}{PrR.} \frac{1}{r} \frac{d}{dr} (rR_{vt}) - 1.6 \frac{d}{dr} \left(\sqrt{(R_{22})l} \frac{d}{dr} R_{vt} \right) - 0.12 \frac{d}{dr} \left((\sqrt{2})Kl \frac{d}{dr} R_{vt} \right) - 2 \frac{R_{\omega}}{R.} R_{\omega t} = 0; \quad (18)$$

$$R_{12} \frac{d\Theta}{dr} - \frac{1}{\int_0^1 Ur dr} R_{11} + R_{vt} \frac{dU}{dr} + 0.48 \sqrt{(Pr)K} \frac{R_{vt}}{l} + \pi \frac{1}{PrR.} \frac{R_{vt}}{l^2} - \frac{1}{PrR.} \frac{1}{r} \frac{d}{dr} \left(r \frac{d}{dr} R_{vt} \right) - 1.6 \frac{1}{r} \frac{d}{dr} \left[r \left(\sqrt{(R_{22})l} \frac{d}{dr} R_{vt} \right) \right] = 0; \quad (19)$$

$$R_{23} \frac{d\Theta}{dr} + \frac{1}{\int_0^1 Ur dr} R_{13} + 0.48 \sqrt{(Pr)K} \frac{R_{\omega t}}{l} + \pi \frac{1}{PrR.} \frac{R_{\omega t}}{l^2} - \frac{1}{PrR.} \left[\frac{1}{r} \frac{d}{dr} (rR_{\omega t}) - \frac{1}{r^2} R_{\omega t} \right] - 1.6 \left[\frac{d}{dr} \left(\sqrt{(R_{22})l} \frac{d}{dr} R_{\omega t} \right) - \frac{2}{r} \sqrt{(R_{22})l} \frac{d}{dr} R_{\omega t} \right] + 2 \frac{R_{\omega}}{R.} R_{\omega t} = 0; \quad (20)$$

$$2R_{vt} \frac{d\Theta}{dr} + \frac{2}{\int_0^1 Ur dr} R_{vt} + \frac{3}{2} \pi \frac{1}{R.} \frac{R_{vt}}{l^2} + 0.1485 Pr^{1/3} K \frac{R_{vt}}{l} - \frac{1}{PrR.} \frac{1}{r} \frac{d}{dr} (rR_{vt}) - \frac{1}{r} \frac{d}{dr} \left[r \left(\sqrt{(R_{22})l} \frac{d}{dr} R_{vt} \right) \right] = 0. \quad (21)$$

When closing this system for correlations, involving pressure pulsations and temperature fluctuation derivatives, as well as for dissipative functions, the Kolovandin approximations are used [8]

$$\frac{1}{\rho} \left\langle p \frac{\partial t}{\partial x_i} \right\rangle = \beta^{wt} \frac{\sqrt{E}}{L} \langle u_i t \rangle; \quad (22)$$

$$2\lambda \left\langle \frac{\partial u_0}{\partial x_k} \frac{\partial t}{\partial x_k} \right\rangle = \gamma_1^{wt} \lambda \frac{\langle u_i t \rangle}{L^2}; \quad (23)$$

$$2\lambda \left\langle \frac{\partial t}{\partial x_k} \frac{\partial t}{\partial x_k} \right\rangle = \gamma_1' \lambda \frac{\langle t^2 \rangle}{L^2} + \gamma' \sqrt{E} \frac{\langle t^2 \rangle}{L}; \quad (24)$$

where

$$\beta^{wt} = 0.48 \sqrt{(Pr)}; \quad \gamma_1^{wt} = \pi; \quad \gamma_1' = \frac{3}{2} \pi Pr; \quad \gamma' \approx 0.1485 Pr^{1/3}.$$

By analogy with (14) and (15), for the functions

describing turbulent diffusion of second moment and diffusion due to pressure pulsations, the following approximations are suggested

$$\frac{\partial}{\partial x_k} \langle u_k u_i t \rangle = -B_2^{wt} \frac{\partial}{\partial x_k} \left[\sqrt{\langle u_k^2 \rangle} L \frac{\partial}{\partial x_k} \langle u_i t \rangle \right]; \quad (25)$$

$$\frac{1}{\rho} \frac{\partial}{\partial x_i} \langle p t \rangle = -B_2^{wt} \frac{\partial}{\partial x_k} \left[\sqrt{(2E)} L \frac{\partial}{\partial x_i} \langle u_i t \rangle \right]; \quad (26)$$

$$\frac{\partial}{\partial x_k} \langle u_k t^2 \rangle = -B_1^{wt} \frac{\partial}{\partial x_k} \left[\sqrt{\langle u_k^2 \rangle} L \frac{\partial}{\partial x_k} \langle t^2 \rangle \right], \quad (27)$$

where the coefficients $B_1^{wt} = 1.6$, $B_2^{wt} = 0.12$, $B_1^{wt} = 1$ are determined numerically from the best correlation between the predicted functions and experimental data of Ibragimov *et al.* [9], Tanimoto *et al.* [10].

Equations (17)–(21) are solved at the boundary conditions

$$\Theta|_{r=1} = R_{vt}|_{r=1} = R_{vt}|_{r=1} = 0; \quad (28)$$

$$\frac{d\Theta}{dr} \Big|_{r=0} = \frac{d}{dr} R_{vt} \Big|_{r=0} = \frac{d}{dr} R_{vt} \Big|_{r=0} = 0.$$

The method of solution and computation algorithm are similar to those given above for the dynamic characteristics.

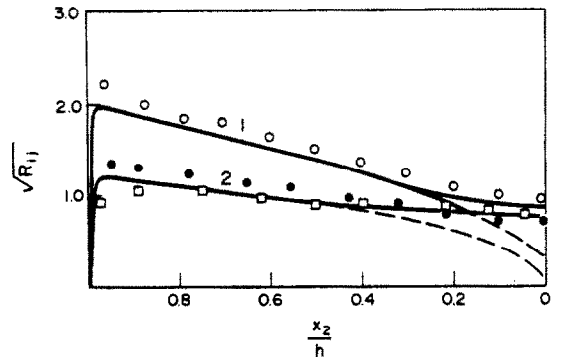


FIG. 1. An effect of turbulent diffusion on normal stress distribution at $R. = 5535$ (1, prediction, R_{11} ; 2, prediction, $R_{22} = R_{33}$. ----, $B_1 = B_2 = 0$; \circ , experiment R_{11} ; \square , experiment [5] R_{22} , \circ , experiment [5] R_{33}).

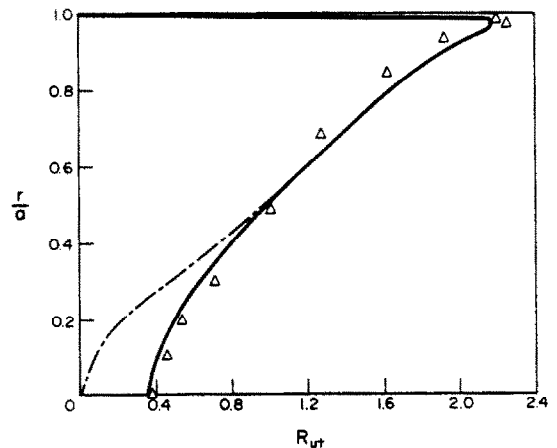


FIG. 2. Contribution of turbulent diffusion to distribution of longitudinal pulsation heat fluxes (—, prediction at $B_1 \neq 0$ and $B_2 \neq 0$; ---, prediction at $B_1 = B_2 = 0$; Δ , experiment [9] $R_{mean} = 32000$).

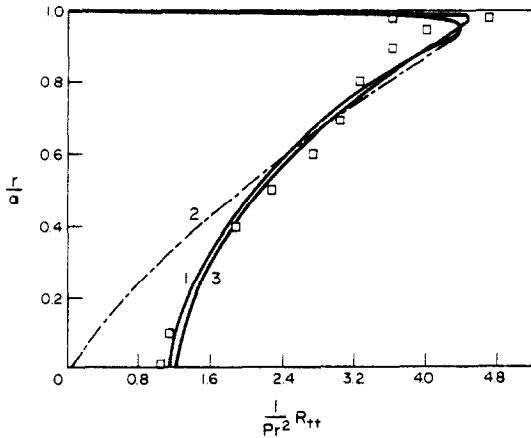


FIG. 3. An effect of turbulent diffusion on temperature fluctuation distribution (1, prediction at $R_w = 10^3$; 2, prediction at $R_w = 10^3$ and $B_1 = B_2 = 0$; 3, prediction at $R_w = 2828$; \square , experiment [10], $R_w = 10^3$).

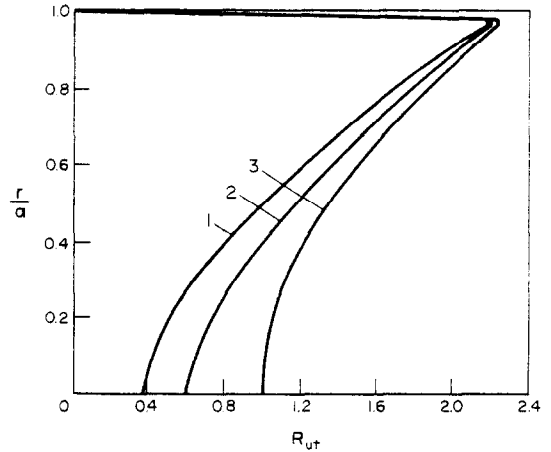


FIG. 6. Contribution of rotation to distribution of longitudinal pulsation heat fluxes at $R_w = 10^3$ (1, $R_w = 0$; 2, $R_w = 5 \times 10^3$; 3, $R_w = 10^4$).

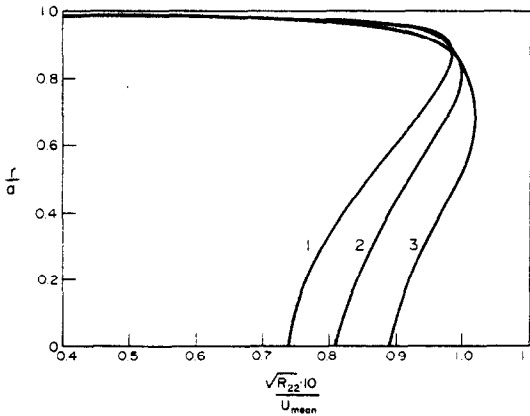


FIG. 4. Contribution of rotation to distribution of transverse velocity pulsations ($R_w = 10^3$; 2, $R_w = 5 \times 10^3$; 1, $R_w = 0$; 3, $R_w = 10^4$).

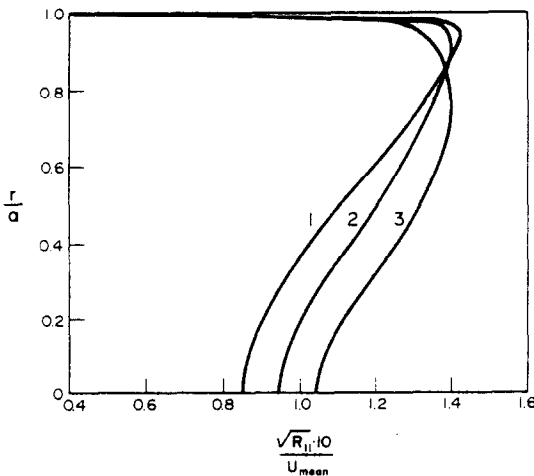


FIG. 5. Contribution of rotation to distribution of longitudinal velocity pulsations at $R_w = 10^3$ (1, $R_w = 0$; 2, $R_w = 5 \times 10^3$; 3, $R_w = 10^4$).

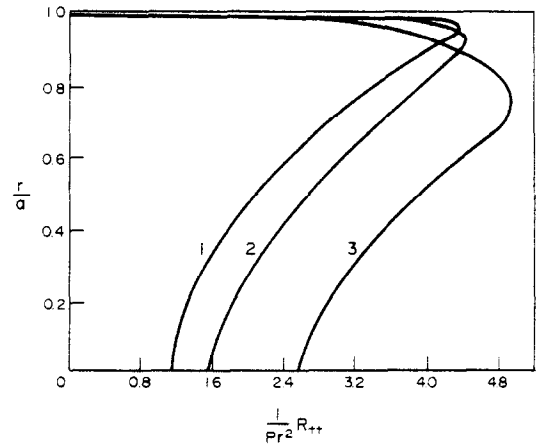


FIG. 7. An effect of rotation on distribution of temperature fluctuations in a tube section at $R_w = 10^3$ (1, $R_w = 0$; 2, $R_w = 5 \times 10^3$; 3, $R_w = 10^4$).

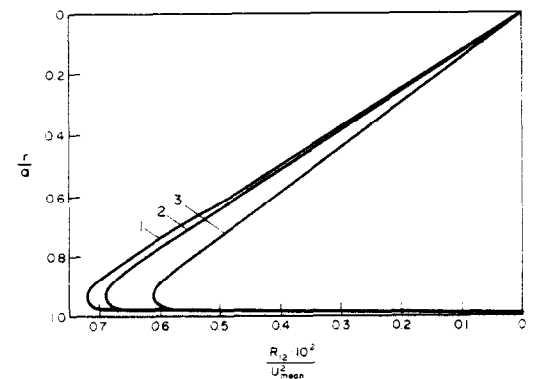


FIG. 8. Distribution of tangential friction in a tube section at $R_w = 10^3$ and different Reynolds numbers for rotation (1, $R_w = 0$; 2, $R_w = 5 \times 10^3$; 3, $R_w = 10^4$).

The analysis of numerical results reveals that the profiles of averaged velocity and temperature become less continuous with increase in the rotation Reynolds number, and this change is the more, the less is R_w as compared to R_w . Correlation R_{23} equals zero like to the case when rotation is not taken into consideration.

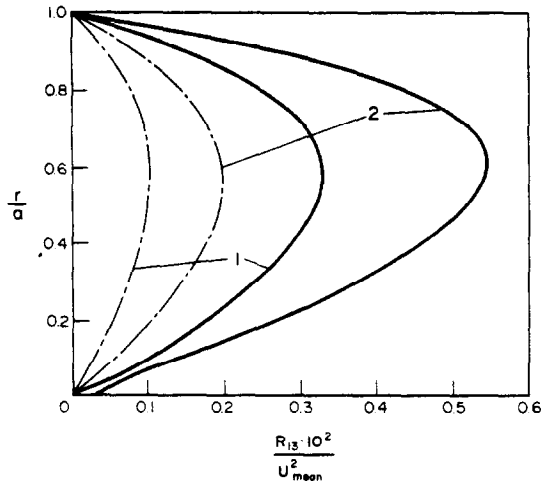


FIG. 9. Contribution of rotation to correlation R_{13} (---, $R = 10^3$; —, $R = 2828$; 1, $R_w = 5 \times 10^3$; 2, $R_w = 10^4$).

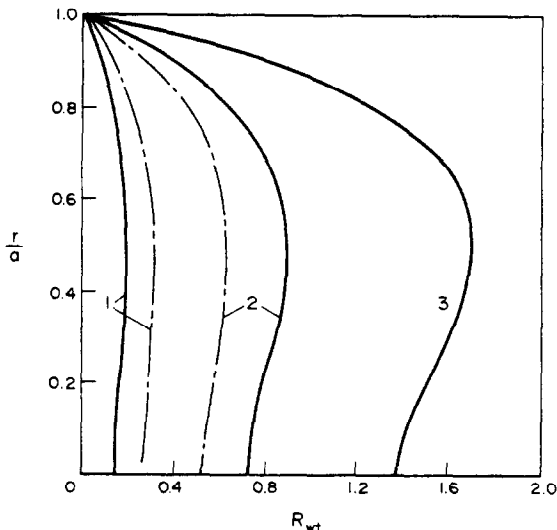


FIG. 10. An effect of rotation on distribution of tangential pulsation heat flux R_w (---, $R = 10^3$; —, $R = 2828$; 1, $R_w = 10^3$; 2, $R_w = 5 \times 10^3$; 3, $R_w = 10^4$).

Functions R_{22} and R_{33} are practically the same over the entire flow. Figures 1–3 show distribution of pulsation energy components, longitudinal pulsation heat flux and mean square temperature fluctuations at

$R_{\omega} = 0$ from which it follows that with neglect of diffusion terms ($B_1 = B_2 = B_1' = B_2' = B_1'' = B_2'' = 0$) the values of these functions in the central channel section are markedly underestimated. It was to be expected from the measurement results of Laufer [11] on balance of the pulsation energy equation according to which the turbulent diffusion and pressure diffusion do not balance each other in this region. The functions R_{11} , R_{22} , R_{33} , R_w and R_{π} (Figs. 4–7) increase in a central region and diminish at a wall with R_{ω} growth. Maxima of these functions displace closer to the tube axis with R_{ω} increase. Correlation R_{12} , characterizing turbulent friction, decreases practically over the entire flow with R_{ω} growth (Fig. 8). A transverse pulsation heat flux slightly increases in the tube centre and decreases near the wall as far as R_{ω} grows. Functions R_{13} and R_w at $R_{\omega} = 0$ are equal to zero and appreciably increase with R_{ω} . In this case the maxima displace closer to the wall (Figs. 9–10).

REFERENCES

1. H. Schlichting, *Entstehung der Turbulenz*. Springer, Berlin (1959).
2. V. B. Levin, On a stabilizing effect of flow rotation on turbulence. *Teplofiz. Vysok. Temper.* 2(6), 892–900 (1964).
3. I. Rotta, Statistische Theorie nichthomogener Turbulenz. *Z. Phys.* 129, 547–572 (1951).
4. S. Donaldson, Calculation of turbulent shear flows for atmospheric and vortex motions, *AIAA JI* 10(1), 4–12 (1972).
5. G. Comte-Bellot, *Ecoulement Turbulent Entre Deux Pairs Paralleles*. Dunod, Paris (1965).
6. R. E. Bellman and R. E. Kalaba, *Quasilinearization and Nonlinear Boundary-Value Problems*. The Rand Corp., New York (1965).
7. B. P. Demidovich, I. A. Maron and E. Z. Shuvalova, *Numerical Methods of Analysis*. Izd. Nauka, Moscow (1967).
8. B. A. Kolovandin, Prediction of basic heat transfer characteristics in turbulent shear flows, in *Collected papers, Heat and Mass Transfer*. P.I. Izd. Energiya, Moscow (1968).
9. M. Kh. Ibragimov, V. N. Subbotin and G. S. Taranov, Determination of relationship between velocity and temperature pulsations in a turbulent air flow in a tube, *Dokl. Akad. Nauk. SSSR* 183(5), 1032–1035 (1968).
10. S. Tanimoto and T. I. Hanratty, Fluid temperature fluctuations accompanying turbulent heat transfer in a pipe, *Chem. Engng Sci.* 18, 307–311 (1963).
11. I. Laufer, The structure of turbulence in fully developed pipe flow, *Nat. adv. Com. Aeronaut., Tech. Rep.* 1174, pp. 1–18 (1954).

DISTRIBUTION DES CARACTERISTIQUES STATISTIQUES DYNAMIQUES ET THERMIQUES DANS DES ECOULEMENTS TURBULENTS INCOMPRESSIBLES ET NON-ISOTHERMES A L'INTERIEUR D'UN TUBE CIRCULAIRE EN ROTATION AUTOUR DE SON AXE

Résumé—On considère dans l'écoulement forcé incompressible à l'intérieur d'un tube, l'effet de la rotation du tube cylindrique autour de son axe, sur les distributions de vitesse et de température moyennes aussi bien que sur les composantes des tensions de Reynolds, des flux de chaleur turbulents et sur la valeur quadratique moyenne des fluctuations de température. L'étude est effectuée par résolution numérique du système d'équations non-linéaires aux dérivées partielles. On présente une discussion des résultats obtenus.

DIE VERTEILUNG DYNAMISCHER UND THERMISCHER STATISTISCHER
KENNGRÖSSEN FÜR TURBULENTE, NICHT-ISOTHERME, INKOMPRESSIBLE
STRÖMUNGEN IN ZYLINDRISCHEN, UM IHRE ACHSE ROTIERENDEN ROHREN

Zusammenfassung — Für erzwungene, inkompressible Strömungen in einem Rohr wird der Einfluß einer Rotation um die Rohrachse auf die Verteilung der mittleren Geschwindigkeit und Temperatur sowie auf die Tensorcomponenten der Reynolds-Spannungen, die Wärmestromschwankungen und die Wurzel aus dem Mittelwert des Quadrats der Temperaturschwankungen untersucht. Die Untersuchung wird mit Hilfe einer numerischen Lösung eines Systems nichtlinearer Differentialgleichungen durchgeführt. Die Ergebnisse werden diskutiert.

РАСПРЕДЕЛЕНИЕ ДИНАМИЧЕСКИХ И ТЕПЛОВЫХ СТАТИСТИЧЕСКИХ
ХАРАКТЕРИСТИК В ТУРБУЛЕНТНЫХ НЕИЗОТЕРМИЧЕСКИХ ПОТОКАХ
НЕСЖИМАЕМОЙ ЖИДКОСТИ ВО ВРАЩАЮЩЕЙСЯ ОТНОСИТЕЛЬНО
СОБСТВЕННОЙ ОСИ ЦИЛИНДРИЧЕСКОЙ ТРУБЕ

Аннотация — Рассматривается влияние вращения цилиндрической трубы относительно собственной оси на распределение осреднённых значений скорости, температуры, а также компонент тензора реинольдсовых напряжений, пульсационных тепловых потоков и среднеквадратичного значения пульсаций температуры в вынужденном потоке несжимаемой жидкости через трубу. Исследование проводилось путем численного решения системы нелинейных дифференциальных уравнений. Приводится обсуждение полученных результатов.